Dynamic Vertical Triplet Energies: A metric for predicting triplet energy transfer

Mihai V. Popescu[a*], Robert S. Paton[a*]

[a]Department of Chemistry, Colorado State University, Ft. Collins, Colorado 80523-1872, United States

ABSTRACT: Visible light energy transfer catalysis has emerged in recent years as an attractive synthetic method for accessing high-energy intermediates, leading to the discovery of novel reactivity modes inaccessible via thermal methods. Computational methods have played a crucial role in understanding and predicting energy transfer catalysis, bypassing the need for complex and laborious photophysical measurements. Specifically, adiabatic triplet energies have been used as a predictive tool in the design of substrates amenable to sensitization, as well as a mechanistic tool. However, this approach fails to accurately predict the likelihood of triplet energy to molecules that undergo large structural changes upon excitation, and provides qualitatively incorrect predictions of *E/Z*-isomerism under energy transfer catalysis. Here, we introduce a new metric, *dynamic vertical triplet energies* (D_VTE), based on the evaluation of change in vertical energy gaps throughout direct dynamics trajectory simulations. This approach improves the predictive capabilities of density functional theory computations and provides further support for the "*hot-band*" mechanism of energy transfer. We demonstrate excellent performance, with R^2 = 0.96 and a mean absolute error (MAE) of 2.1 kcal/mol, for a collection of 20 small organic molecules, whereas the traditional adiabatic model performs significantly worse (R^2=0.58, MAE = 8.3 kcal/mol). We anticipate this approach will be valuable for predicting *E/Z* isomerization triplet energies, for which currently there is no available computational protocol.

Introduction

Triplet-state reactivity has found extensive applications in chemical synthesis, unlocking novel modes of reactivity inaccessible to closed-shell molecules in their ground singlet state. Traditionally, UV-light has been the primary means of harnessing triplet-state chemistry. However, the emergence of visible light energy transfer catalysis has yielded numerous practical advantages,[1] including enhanced reaction yields and improved compatibility with various functional groups.[2] This technology is harnessed by a surge of new synthetic methods,[1] spanning from the exploration of novel reactivity pathways to the synthesis of intricate three-dimensional structures[3] and medicinally significant fragments,[4] asymmetric transformations,[5][6] as well as deracemization reactions[7] and *de-novo photo*-enzymes,[8] but has also impacted fields beyond synthetic chemistry. For instance, in the realm of photoaffinity labeling and materials, this technology has demonstrated remarkable potential.[9] Undoubtedly, the significance of visible light energy transfer catalysis in synthetic methodologies cannot be overstated.

To facilitate the progress of energy transfer applications, a crucial prerequisite is a comprehensive understanding of the triplet energy levels of both the donor and acceptor molecules. Experimentally, these values can be obtained through various spectroscopic techniques, such as phosphorescence spectra analysis by assigning the (0,0) transition energy and magnetically perturbed $S_0 \rightarrow T_1$ absorption spectroscopy, or via a series of quenching experiments.[1][10] Unfortunately, the determination of triplet energies often necessitates specialized equipment that are not readily available in most synthetic laboratories. Additionally, specific expertise is often required for the accurate interpretation and deconvolution of phosphorescence spectra, or the sample itself may exhibit poor photoemissive properties.

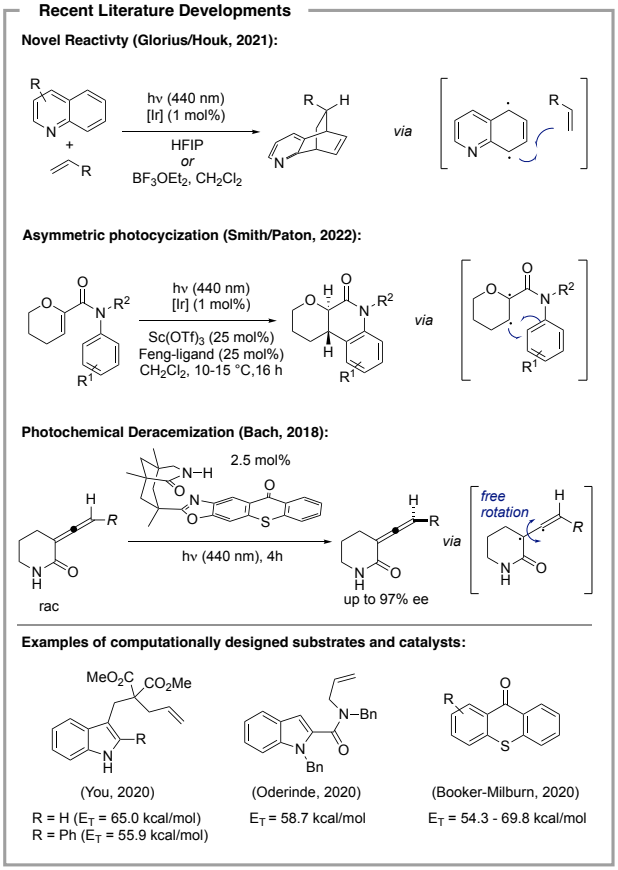

Scheme 1. Recent examples of visible energy transfer applications in synthetic methodology and selected examples of computational designed substrates and catalysts.

In recent years, computational methods employing quantum chemistry (e.g. density functional theory, DFT) have emerged as a valuable approach to address these limitations in the determination of triplet energies.[1] By employing computationally determined *adiabatic* triplet energies (describing the energetic difference between singlet and triplet minima, fully optimized on their respective potential energy surfaces), great strides have been made in accelerating chemical discoveries within this rapidly evolving field. Computational approaches using DFT have found broad applications, including the design of substrates and catalysts tailored for visible light energy transfer applications (Scheme 1),[3h,4a,11] as well as facilitating mechanistic studies.[12] While the adiabatic energy transfer model has demonstrated great success, for systems that are structurally flexible or with highly distorted triplet structures, qualitative explanations of energy transfer catalysis and quantitative predictions of triplet energies may nonetheless fail (see below). To address these shortcomings, this work will introduce an alternative metric based on dynamically evaluating the singlet-triplet gap, aiming to provide a more robust understanding of the underlying processes.

Limitations of the adiabatic model

The prevailing consensus is that energy transfer in solution occurs through the Dexter mechanism, wherein sensitization is explained as a simultaneous intermolecular electron transfer event between donor and acceptor molecules (Figure 1, Eq. 1).[1] Dexter's equation,[13][14] provides a means to assess the rate of energy transfer (k_q) as a function of spectral overlap integral *J*. It is generally accepted that the rate of sensitization primarily relies on the contributions of *J*, and for exothermic processes, a substantial spectral overlap is expected. Consequently, in exothermic reactions, the reaction rate is anticipated to approach the diffusion limit, indicating a rapid and efficient energy transfer. This fundamental assumption also forms the basis of how triplet energies are assigned from quenching experiments.[1]

For ethene, the *computed* adiabatic triplet energy has been reported as 68.8 kcal/mol using high-level Coupled Cluster theory, CCSD(T), extrapolated to the complete basis set (CBS) limit.[15] Using this adiabatic value (as is commonly practiced), it would be expected that with common sensitizers such as benzene (T_E = 84 kcal/mol),[16] acetone (T_E = 81 kcal/mol),[10] and acetophenone (T_E = 74 kcal/mol)[10] energy transfer should proceed in a highly exothermic fashion, with quenching rate constants close to the diffusion limit. To the best of our knowledge, direct energy transfer to non-conjugated alkenes has not been successfully reported in the literature. Evidently, the thermodynamic favorability of energy transfer considering a substrate's adiabatic energy gap does not guarantee sensitization will take place.

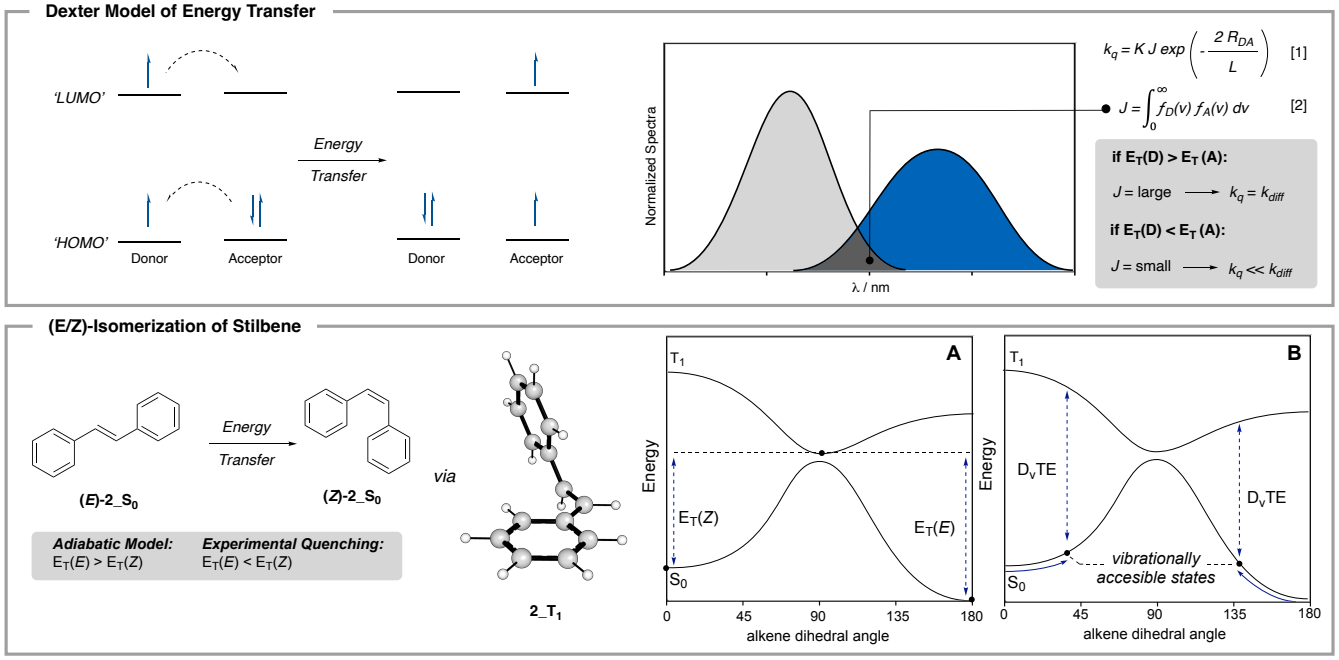

Figure 1: (Top) Mechanism of Dexter energy-transfer, where k_q is the rate of quenching, *K* describes the orbital interaction between the donor and acceptor, *J* represents the spectral overlap integral (Eq. 2), and R_{DA}/L is a measure of the distance between the donor and acceptor molecules; (Bottom) Potential energy surface for the *E/Z*-isomerization of stilbene (A) under the adiabatic mechanism, (B) under the hot-band model.

Further limitations of the reliance on adiabatic triplet energies are apparent when scrutinizing the *E/Z*-isomerization of alkenes, a pivotal process in both synthetic chemistry and biological pathways.[17][18] In recent years, there has been a notable surge in interest in visible light energy transfer as a method for converting the thermodynamically stable *E*-alkenes into the thermodynamically less stable *Z*-isomer, a process that is not possible thermally.[17] Stilbene (**2**), a prototypical substrate for studying *E/Z*-isomerism (Figure 1), has been a focal point in both experimental and computational investigations.[18] Experimental and

computational studies show that a 90˚ dihedral twist occurs in the relaxed triplet state geometries of alkenes, reducing spin-pair repulsion, as observed in stilbene and other alkenes.[1][17] The *E*-isomer, being thermodynamically more stable in the ground state, has a higher adiabatic triplet energy than the *Z*-isomer, since the optimized triplet structure is common to both. However, the selective isomerization of the *E*-isomer to the *Z*-isomer is observed experimentally using sensitizers with appropriate triplet energies.[17] This discrepancy between the adiabatic triplet energies and observed isomerization outcomes underscores the inadequacy of relying solely on adiabatic models when exploring intricate, yet fundamental, processes such as *E/Z*-isomerization. Recently Kerzing and Gilmour have arrived at a similar conclusion, using a combination of in-depth photophysical and computational methods, suggesting that the triplet energy is located somewhere between the adiabatic and vertical gaps.[17b] In their groundbreaking work, they show that triplet energies computed vertically from the S_0 minima qualitatively align with experimental observations, however, they still vastly overestimate tier values.

These observations prompted us to reevaluate the traditional understanding and approach to modeling triplet energies. Insight into the discrepancy between adiabatic triplet energies and triplet energies determined by quenching rates can be obtained by studying endothermic processes. While quenching by exothermic energy transfer is expected to happen with rates close to the diffusion limit, endothermic processes are expected to follow the Sandros-Boltzmann equation [3]:

$$k_q = \frac{k_d}{1 + \exp\left[-\frac{[\mathrm{E(D)} - \mathrm{E(A)}]}{\mathrm{RT}}\right]} \qquad [3]$$

where, k_q is the bimolecular quenching rate constant, k_d is the diffusion rate, E(D) is the triplet energy of the donor, E(A) is the triplet energy of the acceptor, T is the reaction temperature and R is the universal gas constant.[19] This equation serves as the foundation for evaluating experimental triplet energies based on quenching studies, as most systems conform to this relationship. While this model has been well established for many chemical systems, molecules such as *Z*-stilbene have been found to deviate in the endothermic regime.[20] To explain this "non-classical" behavior, proposals involving the notions of "non-vertical" energy transfer gained popularity within the photochemical community.[20] Despite their popularity, these explanations fundamentally challenge the Franck-Condon principle.

An alternative view is the “hot-band” mechanism, where energy transfer to molecules in their ground state occurs through vertical excitation along a vibrational normal mode, leading to a reduction in the energetic separation of the S_0 and T_1 hypersurfaces (Figure 1,B). This explanation maintains elegance without violating the Franck-Condon principle. Wagner and Scheve, studying the “*non-vertical*” sensitization to biphenyl in 1977, reached a similar conclusion but argued that "better potential energy diagrams are required before the original concept of non-vertical energy transfer needs to be completely replaced by the hot-band model".[21] Motivated by Wagner and Scheve’s statement, we hypothesized that advances to algorithms and hardware since their studies make these models now tractable for computational investigation. The work to be described grew out of this assumption.

Dynamic evaluation of triplet energies

The hot-band model stipulates that sensitization proceeds via vertical excitation along vibrational normal modes. Previous investigations of non-vertical energy transfer mechanisms have predominantly focused on interpolating and quantifying the curvature of the potential energy surfaces, with particular emphasis on replicating the shape of the Sandros equation.[22] Here, we propose a different approach by directly extracting the relationship between the S_0 and T_1 excited states from direct dynamics trajectory simulations with DFT. We turned to quasiclassical MD trajectory calculations[23] to sample vibrational motion and to assess the distribution of vertical triplet energies over the timeframe of the simulation(s). These trajectories are initiated in the region of the ground state minimum. Our approach does not explicitly consider the minimum energy structure on the triplet state surface.

Due to the high computational demand of performing direct dynamics trajectories at the DFT level of theory, we adopted a practical approach to balance quantitative accuracy with computational cost. Benchmarking studies against high-level Coupled Cluster calculations of adiabatic triplet energies for several organic molecules indicated the M06-2X/6-31G(d)//M06-2X/MIDI! provides very similar results (MAE = 1.5 kcal/mol) with no appreciable degradation in performance compared to using quadruple-ζ basis sets (MAE = 1.2 kcal/mol) (See Supporting Information).[24] Previous studies have shown that quasiclassical MD trajectories with the MIDI! basis set are sufficient to provide accurate results when evaluating ensemble-averaged molecular properties.[25] In this work, simulations were performed at the M06-2X/MIDI! level of theory and vertical S_0-T_1 gaps were evaluated on these non-stationary point structures at the M06-2X/6-31G(d) level of theory. We used the MILO package[26] developed by Ess and co-workers, interfaced with Gaussian 16.[27] Taking inspiration from aforementioned related protocols for molecular property prediction harnessing quasiclassical dynamics trajectories, 25 trajectories were employed for each molecule and the S_0-T_1 gap was sampled every 8 fs, with total simulation lengths of 1000 fs.[25] For each of the structures investigated, this computational protocol generates an ensemble of triplet energies that are normally distributed. Details of computational benchmarking studies, investigations into the effect of sample size, and detailed statistical assessments of the resulting datasets are described in the Supporting Information.

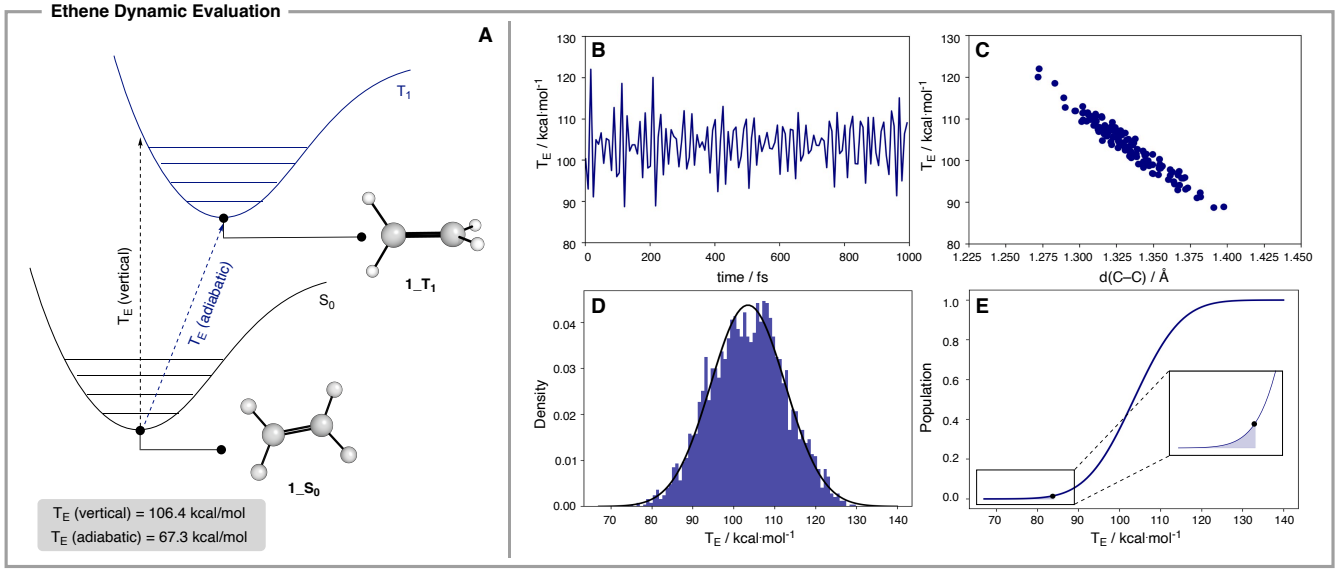

Figure 2: Dynamic evaluation of triplet energies for ethene: (A) cartoon potential energy surface diagram; (B) variation of vertical triplet energy evaluated across a 1000 fs quasiclassical trajectory calculation; (C) vertical triplet energy as a function of C=C bond length; (D) normal distribution of triplet energies across 25 trajectories; (E) normal cumulative distribution of triplet energies across 25 trajectories.

Using ethene as our initial system, the M06-2X/6-31G(d)//M06-2X/MIDI! level of theory gives an electronic (ΔE) adiabatic triplet energy of 67.3 kcal/mol, while the electronic vertical triplet energy from the relaxed ground state singlet geometry is 106.8 kcal/mol. These findings align well with previous literature reports, which indicate adiabatic and vertical triplet energies of 68.8 and 104.1 kcal/mol,[15] respectively, at the CCSD(T)/CBS level of theory. Nevertheless, in experimental studies the triplet energy of ethene was estimated to be 84.0±2.5 kcal/mol using magnetically perturbed S_0-T_1 absorption spectroscopy.[16] Notably, both the adiabatic and vertically determined *ab initio* triplet energies exhibit errors in greater than 16 kcal/mol in comparison to this experimental value. The computed Gibbs free adiabatic triplet energy (ΔG) of 63.1 kcal/mol, which is routinely used in the estimation of triplet energies, was found to perform worse, with an absolute error of 20 kcal/mol.[28]

In evaluating the vertical S_0-T_1 gap, we observed significant fluctuations throughout our simulations (Figure 2B). Collating these computed vertical energies obtained across all 25 simulated trajectories, we found that the S_0-T_1 gap followed a normal distribution ranging from 70 to 130 kcal/mol (Figure 2D). A fitted Gaussian/normal distribution yielded a mean (μ) of 103.5 kcal/mol with a standard deviation (σ) of 9.1. Interestingly, the experimentally determined triplet energy of 84 kcal/mol falls within the range of this dynamically evaluated distribution. To investigate the source of variation in the vertical S_0-T_1 gaps, we examined the correlation between structural parameters and the vertical S_0-T_1 gap. Among those considered, the stretching and compression of the C=C bond exhibits a strong linear inverse correlation (R^2 = 0.95) while other distances, angles, and dihedrals were weakly correlated (Figure 2C). The vibrational distortion of the central C=C bond predominantly contributes to the origin of dynamically distributed triplet energies: for longer distances we expect smaller spin-pair repulsion in the triplet state. The experimental value (84 kcal/mol) corresponds to a central C=C bond stretched to approximately 1.41 Å, representing an increase of 0.08 Å relative to its equilibrium length of 1.33 Å, and closer to the 1.46 Å equilibrium geometry of the T_1 state.

In the framework of the hot-band model, sensitization proceeds through normal mode vibrational distortions. To maximize energy transfer rates, a sufficiently high population of vibrationally distorted species is required, wherein energy transfer is formally exergonic upon encounter complex formation with the sensitizer. To visualize the population as a function of vertical T_E gap, the cumulative normal distribution function provides a more effective representation (Figure 2,E). Based on this analysis, we find that around 1-2% of the total population will have a vertical singlet-triplet energy gap equal to or less than the experimentally determined triplet energy of 84 kcal/mol.

Understanding the significance of the tail-end, rather than the mean value, of this distribution can be qualitatively understood within the context of the Dexter overlap integral (eqs 1-2 in Figure 1). Here, the acceptor excitation S_0-T_1 spectrum intersects the donor phosphoresce at the lower energy end of the distribution. The significance of the empirically determined population can be reconciled by comparison with the Sandros-Boltzmann equation [3].[20] Using this equation, when the triplet energy of the donor molecule matches the acceptor, the rate of quenching occurs at half the diffusion limit. A diffusion rate in the range of 10^{10}-10^{11} $M^{-1}s^{-1}$ depending on the solvent-medium viscosity, corresponds to a formal activation energy barrier of 3 to 4 kcal/mol at room temperature (from transition state

theory).[29] According to the Boltzmann population equation [4], it is expected that, at any given moment, 0.5-2% of the population (ρ) has enough energy to overcome the "activation energy barrier". This observation aligns well with our simulations, in which the experimentally determined value includes 2% of the overall population. The calculation of triplet energy can be refined by utilizing the cumulative distribution function (CDF) [5], specifically for the population that corresponds to half of the diffusion limit. By extracting the μ and σ parameters from the dynamic ensemble of vertical triplet energy calculations, we can more accurately calculate the triplet energy for the critical population point of half the diffusion limit.

$$\rho = e^{-\frac{\Delta G}{k_B T}} \qquad [4]$$

$$\rho(T_E|\,\mu,\sigma) = \frac{1}{\sigma\sqrt{2\pi}}\int_{-\infty}^{T_E} e^{-\frac{(T_E-\mu)^2}{2\sigma^2}}\,dT_E \qquad [5]$$

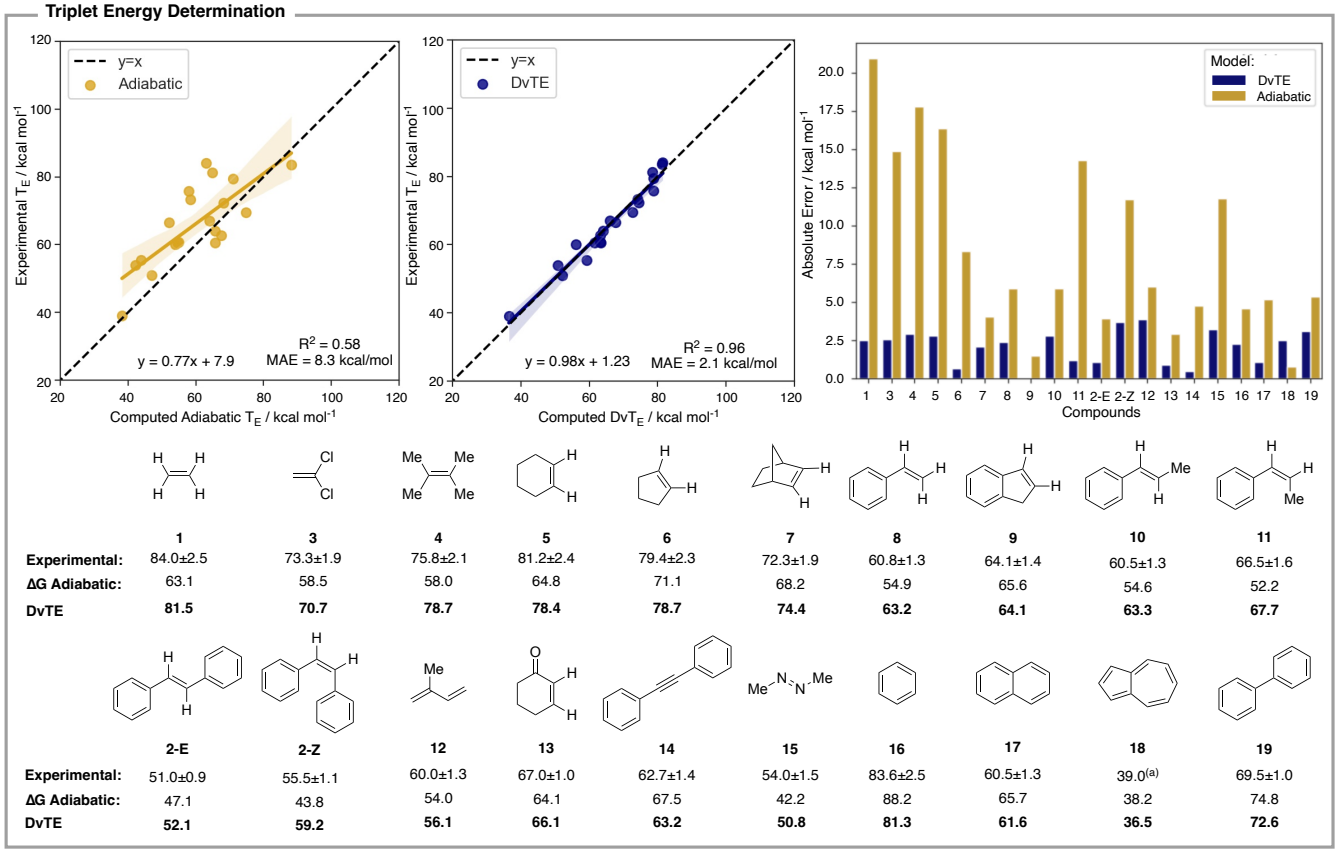

Figure 3: Comparison of computed triplet energies for a series of organic compounds against experimentally determined triplet energies;[16][29] [a]Experimental uncertainty not available; Adiabatic = M06-2X/6-31G(d)//M06-2X/MIDI!; Dynamic vertical Triplet Energy (DvTE) = M06-2X/6-31G(d)//M06-2X/MIDI! trajectories

To investigate the applicability of this approach more broadly, we conducted trajectory simulations for 20 organic substrates with various functional groups, including simple alkenes (**1,3-4**), cyclic alkenes (**5-7,8**), conjugated alkenes (**2,8-9,10-13**), alkynes (**14**), diazines (**15**), as well as aromatic molecules (**16-19**).[16,30] The dynamically-generated results are shown alongside adiabatic triplet energies at the same level of theory and experimentally determined values (Figure 3). Strikingly, the widely used adiabatic model is only modestly correlated with experiment (R^2 = 0.58) with a large mean absolute error (MAE) of 8.3 kcal/mol. Closer examination revealed significant errors for simple alkenes, with ethene displaying the largest error of 20.1 kcal/mol. This trend persisted across all simple alkenes (**1, 3-7**), decreasing for more constrained (i.e., less flexible) structures. The adiabatic prediction for norbornene (**7**) has the lowest error (4.1 kcal/mol), still greater than the experimental uncertainty of 1.5 kcal/mol. Conversely, conjugated alkenes (**2-E/Z, 8-13**) demonstrated improved performance, with errors as low as 1.5 kcal/mol for indene (**9**). However, notable errors persisted, with *E*-β-methyl styrene (**10**) and *Z*-β-methyl styrene (**11**) displaying errors of 6.1 and 14.3 kcal/mol, respectively. Similarly, *Z*-stilbene (**2-Z**) and styrene (**8**) also performed very poorly, with errors of 11.7 and 5.9 kcal/mol, respectively. Dienes such as isoprene (**12**) also gave an error of 6.0 kcal/mol. On the other hand, cyclohexanone (**13**), a common motif in recent visible light energy transfer synthetic methods, was found to also perform reasonably well, leading to an error of 2.9 kcal/mol.[11] Dimethyldiazine (**15**) performed poorly with an 11.8 kcal/mol error. The lowest error was obtained for azulene (**18**), which was found to be 0.8 kcal/mol. Surprisingly, other simple aromatic systems such as benzene (**16**), naphthalene (**17**) and biphenyl (**19**) exhibited errors of 4.6, 5.2 and 5.3 kcal/mol respectively. Collectively, these findings underscore the limitation of

a reliance on the computed adiabatic gap for assessing triplet energies, and highlights potential pitfalls in substrate design for sensitization or as a basis for mechanistic conclusions. Adiabatic analyses with larger basis sets and various levels of theory, including coupled cluster (DLPNO-CCSD(T)/cc-pVTZ//M06-2X/6-31+G(d,p)): R^2 = 0.69; MAE = 8.0 kcal/mol) and multireference methods (NEVPT2:CASSCF/cc-pVTZ//M06-2X/6-31+G(d,p): R^2 = 0.53; MAE = 7.6 kcal/mol) do not change this assessment (see Supporting Information).

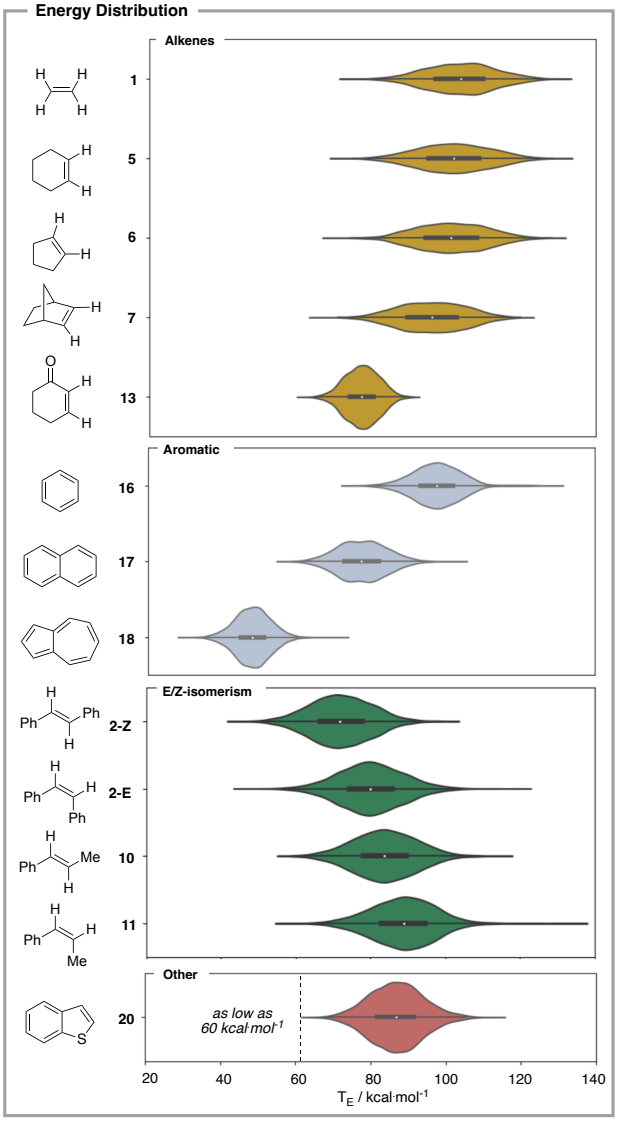

Figure 4: Violin plots of dynamic vertical triplet energy distributions for several alkenes, aromatic and *E/Z*-substituted and other compounds.

In contrast, the dynamic evaluation of triplet energies significantly outperforms adiabatic predictions, yielding a smaller MAE of 2.1 kcal/mol and a correlation coefficient, R^2 = 0.96. A population cutoff 0.8% was empirically-determined. In general, dynamic vertical triplet energies consistently outperform adiabatic measurements, except for azulene (**13**), where DvTE underpredicted the experimental measurements by 2.5 kcal/mol. The largest gain in accuracy was obtained for simple alkene systems, where adiabatic values perform poorly. In all cases, DvTE's were found to significantly outperform the adiabatic values, leading to large decreases in computed errors ranging from 20.9-4.1 kcal/mol down to 2.9-0.4 kcal/mol. The largest deviation was tetramethylethene (**4**: 78.7 kcal/mol) when compared to the experimental value of 75.8±2.1 kcal/mol, however even in this case the computed error of 2.9 kcal/mol was found to be close the experimental reported uncertainty of 2.1 kcal/mol. For other systems where the adiabatic model also performed poorly, such **8**, **12**, **14** and **17** and **19**, DvTE predictions lead to substantial improvements. Additionally, systems that performed well using the adiabatic model, such as **9** and **13** also saw modest improvements in predictive accuracy. Notably, DvTE results are consistent with triplet energies for *E/Z*-isomerization processes, where we correctly identify that isomers (**11**, **2-Z**) possess higher triplet energies than their corresponding *E*-isomers (**10**, **2-E**). Additionally, DvTE values show increased predictive accuracies compared to the adiabatic model, particularly for the *Z*-isomers. For instance, **11** showed a decrease in absolute error from 14.3 to 1.2 kcal/mol, while **2-Z** improved its accuracy from 11.7 to 3.7 kcal/mol.

To gain a deeper understanding of how structural effects influence their vertical triplet energies, the dynamic distributions for several structures are compared in Figure 4. It is apparent that both the centers and the width of these distributions vary across the different compounds both influencing the energy at which energy transfer can occur. For example, the triplet energy distributions for ethene, cyclohexene, cyclopentene and norbornene all have similar width (σ values of 9.1, 9.7, 9.3, and 8.7 kcal/mol), while cyclohexanone, has both a smaller mean (μ = 77.1 kcal/mol) and a much a narrower distribution (σ = 4.6 kcal/mol) as a result of extended π-conjugation. The means of the alkene distributions (103.5, 101.7, 101.1, and 95.9 kcal/mol, respectively) are correlated with their triplet energies, suggesting that the variation is mainly electronic (i.e., rather than dynamic) in nature. Compared to these alkenes, aromatic compounds such as benzene, naphthalene, and azulene produce narrower distributions (σ = 6.7, 6.5, and 4.8, respectively), tightly clustered around the mean. Finally, a comparison of *E* and *Z* alkene-substituted systems revealed that for both stilbene and β-methylstyrene compounds, the differences between their corresponding cis and trans structures were mainly observed in the position of their means. For instance, in *E*-stilbene, the μ is 80.1 kcal/mol with a σ of 8.7, while the *Z*-analogue exhibits a significantly lower μ of 72.1 kcal/mol and a modestly smaller σ of 8.3. A similar pattern is observed in *E*-β-methylstyrene (μ = 88.8 kcal/mol, σ = 8.7) and *Z*-β-methylstyrene (μ = 83.8 kcal/mol, σ = 8.5). These findings align with the ongoing interpretation of *Z*-substituted systems, where the decreased conjugation between the phenyl substituent and the alkene chromophore leads to a substantial change in the mean.

Further applications of the approach

The description of a molecule's triplet energy as emerging from an ensemble of structures sampled by vibrational motions, as opposed to a stationary geometry, has implications beyond triplet energy prediction. Since the effects of changes in temperature and isotopic masses can be captured by the dynamically-averaged triplet energy distribution, we expect this approach will be useful to understand their role in energy transfer processes. Further, we also believe that efforts to develop endergonic energy transfer processes can be informed our approach. For example, recent investigations from the Glorius group highlight the amenability of benzothiophene (**20**) to triplet sensitization using photocatalysts with triplet energies more than 5 kcal/mol lower than the substrate.[31] Both the computed DvTE (70.0 kcal/mol) and adiabatic T_E (73.1 kcal/mol) were found to align well with the experimentally determined T_E of 68.7±0.4 kcal/mol.[32] Examining the vertical T_E distributions revealed a wide range of energies, as indicated by the standard deviation σ = 7.1 for the fitted normal distribution. Within this observed range of vertical triplet energies, values were found to go as low as 60 kcal/mol — a window that falls within the photocatalyst range of 63-65 kcal/mol known to enable sensitization (Figure 4). This suggests that the discovery of substrates with large σ-values in their DvTE distributions may open avenues for discovering and assessing novel endergonic sensitization reactions.

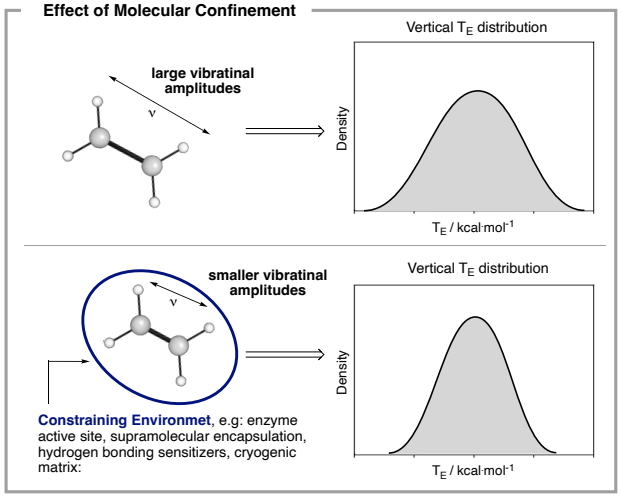

Figure 5: Hypothesized effect of confinement on the distribution of vertical triplet energy gaps.

Building on this interpretation, it becomes apparent the importance of considering triplet energy as a distribution of states rather than a singular value. This perspective opens up discussions about how extrinsic factors might affect the distribution of states by influencing the dynamic behavior of the molecule. A prime example is the effect of molecular confinement. Confining molecules may induce additional anharmonicity in the vibrational modes, impacting the σ-value of the vertical distributions (Figure 5). Notable scenarios include sensitization within the active site of an enzyme,[8] in supramolecular complexes,[33] or in chiral photosensitizers that rely on hydrogen bonding.[6b,d][7] These considerations open the doors to an additional dimension for reaction optimization.

Model limitations and performance

The dynamic approach to triplet energy evaluation gives a pronounced improvement in predicting experimental values (the MAE is reduced from 8.3 kcal/mol to 2.1 kcal/mol), but there are certain practical limitations. One limitation of this model is that it omits contributions from the orbital overlap contributions,[6e][34] while also assuming that the diffusion-limited rate constant is the same for all molecules studied. Further, the computational demand is increased relative to adiabatic calculations using ground-state structures. Under the proposed protocol, 6250 single-point energy calculations are performed on snapshots from quasiclassical trajectory calculations. Moderately large systems like ***Z/E*-2** require approximately 1000 CPU core hours using our computational resources.[35] Despite the current computational protocol not being conducive to high-throughput screening campaigns, we anticipate that ongoing advancements in machine learned potentials may streamline the process for dynamically evaluating triplet energies.[36] Nevertheless, we firmly believe that this new methodology enhances our fundamental understanding of the sensitization process and is well-suited for single-use scenarios where in-depth mechanistic understanding is crucial for designing better sensitization reactions. For instance, using ethene as an example, a 20 kcal/mol error for adiabatic interpretation is significantly high to miss assess the likelihood of ease of energy transfer, and *E/Z*-isomerization would predict the wrong product formation, inconsequential of the chosen level of theory.

CONCLUSIONS

In summary, we have proposed a novel approach and metric for evaluating triplet energies. This metric, based on the hot-band model of energy transfer, offers a significant improvement over the commonly used adiabatic model, reducing the mean absolute error (MAE) from 8.3 kcal/mol to 2.1 kcal/mol. Given the considerable uncertainties associated with adiabatic predictions, we strongly recommend utilizing the computed DvTE instead. Additionally, we envision that the analysis of triplet energies obtained from molecular dynamics as a distribution of states, rather than a singular value, may enable the discovery of new ways of controlling triplet energy, while also facilitating the identification of molecules amenable to endergonic energy transfer.

ASSOCIATED CONTENT

The Supporting Information is available free of charge via the Internet at http://pubs.acs.org. Computational Methods and Workflows, Benchmarking Data, Processed MD data. Python code as well as trajectory files are available at https://github.com/mpv94/DvTE

AUTHOR INFORMATION

Corresponding Authors

Mihai V. Popescu − Department of Chemistry, Colorado State University, Ft. Collins, Colorado 80523-1872, United States; Email: mihai.popecu@colostate.edu
Robert S. Paton − Department of Chemistry, Colorado State University, Ft. Collins, Colorado 80523-1872, United States; orcid.org/0000-0002-0104-4166; Email: robert.paton@colostate.edu

Notes

The authors declare no competing financial interest.

ACKNOWLEDGMENT

RSP acknowledges funding from the NIH (R01 GM151533) and the Alpine high-performance computing resource, jointly funded by the University of Colorado Boulder, the University of Colorado Anschutz, and Colorado State University, and ACCESS through allocation TG-CHE180056.

REFERENCES

(1) (a) Strieth-Kalthoff, F.; James, J. M.; Teders, M.; Pitzer, L.; Glorius, F. Energy Transfer catalysis mediated by visible light: principles., applications, directions. *Chem. Soc. Rev.*, **2018**, *47*, 7190-7202; (b) Strieth-Kalthoff, F.; Glorius, F. Triplet Energy Transfer Photocatalysis: Unlocking the Next Level. *Chem*, **2020**, *6*, 1888-1903; (c) Dutta, S.; Erchinger, J. E.; Strieth-Kalthoff, F.; Kleinmans, R.; Glorius, F. Energy transfer photocatalysis: exiting modes of reactivity. *Chem. Soc. Rev.* **2024**, *53*, 1068-1089.

(2) Yoon, T. P.; Ischay, M. A.; Du, J. Visible light photocatalysis as a greener approach to photochemical synthesis. *Nat. Chem.* **2010**, *2*, 527-532.

(3) Selected examples: (a) Wang, H.; Shao, H.; Das, A.; Dutta, S.; Chan, H. T.; Daniliuc, C; Houk, K. N.; Glorius F. Dearomative ring expansion of thiphenes by bicyclobutanes. *Science*, **2023**, *381*, 75-81. (b) Kleinmans, R.; Pinkert, T.; Dutta, S.; Paulich, T. O.; Keum, H.; Daniliuc C. G.; Glorius F. Intermolecular [2π+2s]-photocycloaddition enabled by triplet energy transfer. *Nature*, **2022**, *605*, 477-482. (c) Ma, J.; Chen, S.; Bellotti, P.; Guo, R.; Schäfer, F.; Heusler, A.; Zhang, X.; Daniliuc, C.; Brown, M. K.; Houk, K. N.; Glorius, F. Photochemical Intermolecular Dearomative Cycloaddition of Bicuclic Azaarenes with Alkenes. *Science*, **2021**, *371, 1338-1345.; (d)* James, M. J.; Schwarz S. L.; Strieth-Kalthoff, F.; Wibbeling, B.; Glorius F. Dearomative Cascade Photocatalysis: Divergent Synthesis through Catalyst Selective Energy Transfer. *J. Am. Chem. Soc.* **2018**, *140,* 8624-8628. (e) Zhu, M.; Zhang, X.; Zheng, C.; You, S. -L. Energy-Transfer-Enabled Dearomative Cycloaddition Reactions of Indoles/Pyrroles via Excited-State Aromatics. *Acc. Chem. Res.* **2022**, *55*, 2510-2525.; (f) Zhu, M.; Huang, X. -L.; Sun, S.; Zheng, C.; You, S. -L. Visible-Light-Induced Dearomatization of Indoles/Pyrroles with Vinylcyclopropanes: Expedient Synthesis of Structurally Diverse Polycyclic Indolines/Pyrrolines. *J. Am. Chem. Soc.* **2021**, *143*, 13441-13449. (g) Zhu, M.; Xu, H.; Zheng, C.; You, S. -L. Visible-Light-Induced Intramolecular Double Dearomative Cycloaddition of Arenes. *Agnew. Chem. Int.* Ed. **2021**, *60*, 7036-7040. (h) Zhu, M.; Zheng, C.; Zhang, X.; You, S. -L. Synthesis of Cyclobutane-Fused Angular Tetracyclic Spiroindolines via Visible-Light-Promoted Intramolecular Dearomatization of Indole Derivatives. *J. Am. Chem. Soc.* **2019**, *141*, 2636-2644.

(4) (a) Oderinde, M. S.; Mao, E.; Ramirez, A.; Pawluczyk, J.; Jorge, C.; Cornelius, L. A. M.; Kempson, J.; Vetrichelvan, M.; Pitchai, M.; Gupta, A.; Gupta, A. K.; Meanwell, N. A.; Mathur, A.; Dhar, T. G. M. Light Photocatalysis for Building Molecular Complexity. *J. Am. Chem. Soc.* **2020**, *142*, 3094-3103. (b) Murray, P. R. D.; Bussink, W. M. M.; Davies, G. H. M.; van der Mei, F. W.; Antropow, A. H.; Edwards, J. T.; D'Agostino, L. A.; Ellis, J. M.; Hamann, L. G.; Romanov-Michailidis, F.; Knowles, R. R. Intermolecular Crossed [2+2] Cycloaddition Promoted by Visible-Light Triplet Photosensitization: Expedient Access to Polysubstituted 2-Oxaspiro[3.3]heptanes. *J. Am. Chem. Soc.* **2021**, *143*, 4055-4063.

(5) For a recent review: Großkopf, J.; Kratz, T.; Rigotti, T.; Bach, T. Enantioselective Photochemical Reactions Enabled by Triplet Energy Transfer. *Chem. Rev.* **2022**, *122*, 1626-1653.

(6) Selected examples: (a) Jones, B. A.; Solon, P.; Popescu, M. V.; Du, J. -Y.; Paton, R.; Smith, M. D. Catalytic Enantioselective 6π Photocyclization of Acrylanilides. *J. Am. Chem. Soc.* **2023**, 145, 171-178. (b) Swords, W. B.; Lee, H.; Park, Y.; Llamas, F.; Skubi, K. L.; Park, J.; Guzei, I. A.; Baik, M. -H., Yoon, T. Highly Enantioselective 6π Photoelectrocyclizations Engineered by Hydrogen Bonding. *J. Am. Chem. Soc.* **2023**, *145*, 27045-27053. (c) Chapman, S. J.; Swords, W. B.; Le, C. M.; Guzei, I. A.; Toste, F. D.; Yoon, T. P. Cooperative Stereoinduction in Asymmetric Photocatalysis. *J. Am. Chem. Soc.* **2022**, 144, 4206-4213. (d) Zheng, J.; Swords, W. B.; Jung, H; Skubi, K. L.; Kidd, J. B.; Meyer, G. J.; Baik, M. -H.; Yoon, T. P., Enantioselective Intermolecular Excited-State Photoreactions Using a Chiral Ir Triplet Sensitizer: Separating Association from Energy Transfer in Asymmetric Phtocatalysis. *J. Am. Chem. Soc.* **2019**, *141*, 13625-13634. (e) Daub, M. E.; Jung, H.; Lee, B. J.; Won, J.; Baik, M. H.; Yoon, T. P. Enantioselective [2+2] Cycloaddition of Cinnamates Esters: Generalizing Lewis Acid Catalysis of Triplet Energy Transfer. *J. Am. Chem. Soc.* **2019**, *141*, 9543-9547. (f) Blum, T. R.; Miller, Z. D.; Bater, D. M.; Guzei, I. A.; Yoon, T. P. Enantioselective photochemistry through Lewis acid-catalyzed triplet energy transfer. *Science*, **2016**, *354,* 1391-1395. (g) Du, J.; Skubi, K. L.; Schultz, D. M.; Yoon, T. P. A Dual-Catalysis Approach to Enantioselective [2+2] Photocylcoadditions Using Visible Light. *Science*, **2014**, *344*, 392-396. (h) Alonso, R.; Bach, T. A chiral Thioxanthone as an Organocatalyst for Enantioselective [2+2] Photochycloaddition Reactions Induced by Visible Light. *Angew. Chem. Int. Ed.* **2014**, *53*, 4368-4371.

(7) Selected examples: (a) Hölzl-Hobmeier, A.; Bauer, A.; Silva, A. V.; Huber, S. M.; Bannwarth, C.; Bach, T. Catalytic deracemization of chiral allenes by sensitized excitation with visible light. *Nature,* **2018**, *564*, 240-243; (b) Kratz, T.; Steinbach, P.; Breitenlechner, S.; Storch, G.; Bannwarth, C.; Bach, T. Photochemical Deracemization of Chiral Alkenes via Triplet Energy Transfer. *J. Am. Chem. Soc.* **2022**, *144*, 10133-101388.

(8) (a) Trimble, J. S.; Crawshaw, R.; Hardy, F. J.; Levy, C. W.; Brown, M. J. B.; Fuerst, D. E.; Heyes, D. J.; Obexer, R.; Green, A. P. A design photoenzyme for enantioselective [2+2] cycloadditions. *Nature*, **2022**, *611*, 709-714; (b) Sun, N.; Huang, J.; Qian, J.; Zhou, T. -P.; Guo, J.; Tang, L.; Zhang, W.; Deng, Y.; Zhao, W.; Wu, G.; Liao, R. -Z.; Chen, X.; Zhong, F.; Wu, Y. Enatioselective [2+2]-cycloadditions with triplet photoenzymes. *Nature*, **2022**, *611*, 715-720.

(9) (a) Seath, C. P.; Burton, A. J.; Sun, X.; Lee, G.; Kleiner, R. E.; MacMillan, D. W. C.; Muir, T. W. Tracking Chromatic State Changes using nanoscale photo-proximity labelling. *Nature*, **2023**, *616*, 574-580. (b) Suzuki, S.; Geri, J. B.; Knutson, S. D.; Bell-Temin, H.; Tamura, T.; Fernández, D. F.; Lovett, G. H.; Till, N. A.; Heller, B. L.;

Guo, J.; MacMillan, D. W. C.; Ploss, A. Photochemical Indentification of Auxiliary Severe Acute Respiratory Syndrome Coronavirus 2 Host Entry Factors Using mMap. *J. Am. Chem. Soc.* **2022**, *144*, 16604-16611. (c) Meyer, C. F.; Seath, C. P.; Knutson, S. D.; Lu, W.; Rabinowitz, J. D.; MacMillan, D. W. C. Photoproximity Labeling of Sialylated Glycoproteins (ClycoMap) Reveals Sialylation-Depndent Regulation of Ion Transport. *J. Am. Chem. Soc.* **2022**, *144*, 23633-23641. (d) Geri, J. B.; Oakley, J. V.; Reyes-Robles, T.; Wang, T.; McCarver, S. J.; White, C. H.; Rodriguez-Rivera, F. P.; Parker Jr., D. L.; Hett, E. C.; Fadeyi, O. O.; Oslund, R. C.; MacMillan, D. W. C. Microenvironment mapping via Dexter energy transfer on immune cells. *Science*, **2020**, *367*, 1091-1097.

(10) Murov, S. L.; Charmichael, I.; Hug, G. L. Handbook of Photochemistry. Marcel Dekker Ink, New York, **1993**.

(11) Elliot, L. D.; Kayal, S.; George, M. W.; Booker-Milburn, K. Rational Design of Triplet Sensitizers for the Transfer of Excited State Photochemistry from UV to Visible. *J. Am. Chem. Soc.* **2020**, *142*, 14947-14956.

(12) Additional selected examples: (a) Münster, N.; Parker, N. A.; van Dijk, L.; Paton, R. S.; Smith, M. D. Visible Light Photocatalysis of 6π Heterocyclization. *Angew Chem. Int. Ed.* **2017**, *56*, 9468-9472 (b) Popescu, M., Parker, N.; Jia, Z.; Solon, P.; Alegre-Requena, J.; Paton, R.; Smith, M. An energy transfer mediated 4π spirocyclization intercepts the Staudinger b-lactam synthesis. *ChemRxiv*, **2023**, DOI:10.26434/chemrxiv-2023-kn7gf; (c) Popescu, M. V.; Mekereeya, A.; Alegre-Requena, J. V.; Paton, R. S.; Smith, M. D. Visible-Light-Mediated Heterocycle Functionalization via Geometrically Interrupted [2+2] Cycloaddition.

(13) Dexter, D. L. A theory of sensitized Luminescence in solids, *J. Chem. Phys.* **1953**, *21*, 836-850.

(14) Balzani, V.; Ceroni, P.; Juris, A. Photochemistry and Photophysics, Wiley-VCH, **2015**.

(15) Nguyen, M. T.; Matus, M. H.; Leser, W. A.; Dixon, D. A. Heats of Formation of Triplet Ethylene, Ethylidene and Acetylene. *J. Phys. Chem. A.* **2008**, *112*, 2082-2087.

(16) Ni, T.; Caldwell, R. A.; Melton, L. A. The Relaxed and Spectroscopic Energies of Olefin Triplets. *J. Am. Chem. Soc.* **1988**, *111*, 457-464.

(17) (a) Neveselý, T.; Wienhold, M.; Molly, J. J.; Gilmour, R. Advances in the E → Z Isomerization of Alkenes Using Small Molecule Photocatalysts. *Chem. Rev.* **2022**, *122*, 2650-2694. (b) Zähringer, T. J. B.; Wienhold, M.; Gilmour, R.; Kerzig, C. Direct Observation of Triplet States in the Isomerization of Alkenylboronates by Energy Transfer Catalysis. *J. Am. Chem. Soc.* **2023**, 145, 21576-21586.

(18) Gordon-Walker, A.; Radda, G. K., Flavin-photosensitized reactions of retinal and stilbene, *Biochem. J.* **1970**, *120*, 673-681.

(19) Sandros, K. Transfer of Triplet State Energy in Fluid Solutions. III. Reversible Energy Transfer. *Acta. Chem. Scand.* **1964**, *18*, 2355-2374.

(20) (a) Hammond, G. S.; Saltiel, J. Mechanism of Photoreactions in Solution. XVIII. Energy Transitions with Nonvertical Transitions. *J. Am. Chem. Soc.* **1963**, 85, 2516-2517. (b) Hammond, G. S.; Saltiel, J.; Lamola, A. A.; Turro, N. J.; Bradsshaw, J. S.; Cowan, D. O.; Counsell, R. C.; Vogt, V.; Dalton, C. Mechanisms of Photochemical Reactions in Solution. XXII.[1] Photochemical cis-trans Isomerization. *J. Am. Chem. Soc.* **1964**, 86, 3197-3217. (c) Saltiel, J.; Townsend, D. E.; Sykes, A. The Quntum Chain Process in the Sensitized Cis-Trans Photoisomerization of 1,3-Dienes. *J. Am. Chem. Soc.* ***1973,*** *95*, 5968-5973.

(21) (a) Yamauchi, S.; Azumi, T. Reinterpretation of "nonvertical" triplet-triplet energy transfer and photoisomerization of stilbene. *J. Am. Chem. Soc.* **1973**, *95*, 2709-2711. (b) Farmilo, A.; Wilkinson, F. Triplet state quenching by ferrocene. *Chem. Phys. Lett.*, **1975**, *34*, 575-580. (c) Wagner, P. J.; Scheve, B. J. Triplet energy transfer. 11. Steric effects in the singlet-triplet transitions of methyl- and chlorobiphenyls. *J. Am. Chem. Soc.* **1977**, *99*, 2888-2892. (d) Bylina, A. Triplet-Triplet energy transfer and the overlap of singlet-triplet bands of sensitizer and acceptor. Remarks on the 'phantom triplet' of stilbene. *Chem. Phys. Lett.* **1968**, *1*, 509-510. (e) Balzani, V.; Bolletta, F.; Scandola, F. Vertical and "Nonvertical" Energy Transfer Processes. A General Classical Treatment. *J. Am. Chem. Soc.* **1980**, 102, 2152-2163.

(22) (a) Lalevée, J.; Allonas, X.; Louërat, F.; Fouassier, J. P. Role of Structural Changes in the Triplet-Triplet Energy Transfer Process to Oxime Derivatives. *J. Phys. Chem. A*, **2022**, *29*, 6702-6709; (b) Frutos, L. M.; Castaño, O. A new algorithm for predicting triplet-triplet energy-transfer activated complex coordinate in terms of accurate potential-energy surfaces. *J. Chem. Phys.* **2005**, *123*, 104108; (c) Zapata, F.; Marrazi, M.; Castaño, O.; Acuña, A. U.; Frutos, L. M. Definition and determination of the triplet-triplet energy transfer reaction coordinate. *J. Chem. Phys.* **2014**, *140*, 034102; (d) Frutos, L. M.; Castaño, O. A theory of non-vertical triplet energy transfer in terms of accurate potential energy surfaces: The transfer reaction from π,π* triplet donors to 1,3,5,7-cyclooctatetraene. *J. Chem. Phys.* **2004**, *120*, 1208-1216.

(23) (a) Sun, X.; Wang, H.; Miller, W. H. On the semiclassical description of quantum coherence in thermal rate constants. *J. Chem. Phys.* **1998**, 109, 4190-4200; (b) Thoss, M.; Wang, H.; Semiclassical Description of Molecular Dynamics Based on Initial-Value Representation Methods. *Annu. Rev. Phys. Chem.* **2004**, *55*, 299-332.

(24) (a) Zhao, Y.; Truhlar, D. G. The M06 suite of density functionals for main group thermochemistry, thermochemical kinetics, noncovalent interactions, excited states and transition elements: two new functionals and systematic testing of four M06-class functionals and 12 other functionals. *Theor. Chem. Acc.* **2008**, *120*, 215-241; (b) Easton, R. E.; Giesen, D. J.; Welch, A.; Cramer, C. J.; Truhlar, D. G. The MIDI! Basis set for quantum mechanical calculations of molecular geometries and partial charges. *Theor. Chem. Acc.* **1996**, *93*, 281-301; (c) Ditchfield, R.; Hehre, W. J.; Pople, J. A. Self-Consistent Molecular Orbital Methods. 9. Extended Gaussian-type basis for molecular-orbital studies of organic molecules. *J. Chem. Phys*. **1971**, *54*, 724.

(25) Kwan, E. E.; Liu, R. Y. Enhancing NMR prediction for Organic Compounds Using Molecular Dynamics. *J. Chem. Theory Comput.* **2015**, *11*, 5083-5089.

(26) Milo, revision 1.0.3., Teynor, M. S.; Wohlgemuth, N.; Carlson, L.; Huang, J.; Pugh, S. L.; Grant, B. O.; Hamilton, R. S.; Carlsen, R.; Ess, D. H., Brigham Young University, Provo UT, **2021** (https://github.com/DanielEss-lab/milo).

(27) Gaussian 16 version C.01 was utilized for all quantum chemical calculations. For a comprehensive methodology breakdown please refer to the Supporting Information.

(28) Benchmarking data (see Supporting Information) shows that adiabatic electronic energy correlates marginally better with experimentally determined triplet energies across a wide range of levels of theory. However, as the standard of the field is to utilize Gibbs free energy in the estimation of triplet energies, we will utilize adiabatic Gibbs free energy for the remainder of the study.

(29) Besora, M.; Maseras, F. Microkinetic modelling in homogeneous catalysis. *WIREs*, **2018**, *8*, e1372.

(30) (a) Herkstroeter, W. G. The Triplet Energies of Azulene, b-Carotene, and Ferrocene. *J. Am. Chem. Soc.* **1975**, *97*, 4161-4167; (b) De Mayo, P.; Nicholas, A. A.; Tchir, M. F. Photochemical synthesis 29.[1,2,3] Photoannelation and cyclohexanone, *Can. J. Chem.* **1970**, *48*, 225-235; (c) Metcalfe, J.; Chervinsky, S.; Oref, I. Singlet-Triplet absorption of azoalkenes. *Chem. Phys. Lett.* **1976**, *15*, 190-192; (d) Wagner, P. J. Conformational Changes Involved in the Singlet-Triplet Transitions of Biphenyl. *J. Am. Chem. Soc.* **1967**, *89*, 2820-2825.

(31) Strieth-Kalthoff, F.; Henkel, C.; Teders, M.; Kahnt, A.; Knolle, W.; Gomez-Suarez, A.; Dirian, K.; Alex, W.; Bergander, K.; Daniliuc, C. G.; Abel, B.; Guldi, D. M.; Glorius, F. Discovery of Unforeseen Energy-Transfer-Based Transformations Using a Combined Screening Approach. *Chem,* **2019**, *8*, 2183-2194

(32) Zander, M. Zur Photolumineszenz von Benzologen des Thiophens. *Z. Naturforsch*. **1985**, *40a*, 497-502.

(33) Gemen, J.; Church, J. R.; Ruoko, T. -P.; Durandin, N; Białek, M. J.; Weißenfels, M.; Feller, M.; Kazes, M.; Odaybat, M.; Borin, V. A.; Kalepu, R.; Diskin-Posner, Y.; Oron, D.; Fuchter, M. J.; Priimagi, A.; Schapiro, I.; Klajn, R. Disequilibrating azoarenes by visible-light sensitization under confinement. *Science*, **2023**, *381*, 1357-1363

(34) (a) Bai, S.; Zhang, P.; Beratan, D. N. Predicting Dexter Energy Transfer Interactions from Molecular Orbital Overlaps. *J. Chem. C.* **2020**, 124, 18956-18960; (b) Skourtis, S. S.; Liu, C.; Antoniou, P.; Virshup, A. M.; Beratan, D. N., Dexter energy transfer pathways. *PANS*, **2016**, 113, 8115-8120; (c)You, Z. -Q.; Hsu, C. -P.; (d) Fleming, G. R., Triplet-triplet energy-transfer coupling: Theory and calculation, *J. Chem. Phys.* **2006**, 124, 044506; (e)You, Z. -Q.; Hsu, C. -P., Theory and calculation for the electronic coupling in excitation energy transfer, *Int. J. Quantum Chem.* **2014**, 114, 102-115; (f) Subotnik, J. E.; Vura-Weis, J.; Sodt, A. J.; Ratner, M. A. Predicting Accurate Electronic Excitation Transfer Rates via Marcus Theory with Boys or Edmiston-Ruedenberg Localized Diabatization. *J. Phys. Chem. A,* **2010**, 114, 8665-8675.

(35) AMD EPYC 7302 16-Core Processors 3.0GHz

(36) (a) Smith, J. S.; Isayev, O.; Roitberg, A. E. ANI-1: an extensible neural network potential with DFT accuracy at force field computational cost. *Chem. Sci.*, **2017,** 8, 3192-3203; (b) Schütt, K. T.; Sauceda, H. E.; Kindermans, P. -J.; Tkatchenko, A.; Müller, K. -R. SchNet – A deep learning architecture for molecules and materials. *J. Chem. Phys.* **2018**, 148, 241722; (c) Young, T. A.; Johnston-Wood, T.; Deringer, V. L.; Duarte, F. A transferable active-learning strategy for reactive molecular force fields. *Chem. Sci.* **2021**, 12, 10944-10955; (d) Li, J.; Lopez, S. A. Machine learning accelerated photodynamics simulations. *Chem. Phys. Rev.* **2023**, 4, 031309; (e) Li, J.; Reiser, P.; Boswell, B. R.; Eberhard, A.; Burns, N. Z.; Friederich, P.; Lopez, S. A. Automatic discovery of photoisomerization mechanisms with nanosecond machine learning photodynamics simulations. *Chem. Sci.* **2021**, *12*, 5302-5314; (f) Feng, Z.; Guo, W.; Kong, W. -Y.; Chen, D.; Wang, S.; Tantillo, D. J. Analogies between photochemical reactions and ground-state post-transition-state bifurcations shed light on dynamical origins of selectivity. *Nat. Chem.* **2024**, 16, 615-623.